Journal of Sound and Vibration (1976) **49**(2), 179–193

PROPAGATION OF GROUND VIBRATION: A REVIEW

T. G. GUTOWSKI AND C. L. DYM

Bolt Beranek and Newman Inc.,
50 *Moulton Street, Cambridge, Massachusetts* 02138, *U.S.A.*

(*Received* 20 *April* 1976, *and in revised form* 20 *July* 1976)

A review of the current state of the art of ground vibration propagation is presented herein. First the theoretical models of vibration attenuation are reviewed and then measurement techniques are discussed. Finally, measurement and theory are combined into predictive models, whose validity is discussed.

1. INTRODUCTION

An important environmental aspect of building and facility design is the evaluation of vibration transmitted to the site, through the ground, from external sources. Such external sources may include highway traffic, surface and subsurface railways, and machinery in nearby locations. To properly predict excitation levels at a building due to such sources, one must be able to predict how much vibration, in terms of both levels and spectra, is transmitted through the ground from the source.

The problem of predicting the transmission of vibration through the ground is complex [1–8]. The reasons for this complexity include the lack of a comprehensive understanding of soil behavior, the difficulty of determining accurate values of soil properties, and the difficulty of modeling precisely the sources of vibration and the resulting near- and far-field behavior. However, in spite of these and other obstacles, it is possible to make reasonable assessments of ground-transmitted vibration through a judicious use of the empirical and theoretical results that are available.

In this paper a review is given of the current state of the art of vibration transmission prediction. It is important to bear in mind that the focus of this paper is not the prediction of levels due to a particular physical source, but rather is it the prediction of the *transmission* of ground vibration signals from any of a number of sources.

The paper is organized as follows. The basic theoretical models for radiation damping (geometrical spreading) and material damping (energy dissipation) are discussed first. Then a précis of current measurement technology and procedure is given. In the next section a review and collation of published measured vibration data is presented, together with empirical attenuation models derived from these data. Finally, a few comments on future research needs are put forward.

2. THEORETICAL RADIATION MODELS†

One first needs to define the source of the vibration. In terms of traffic-induced vibration, for example, it is of particular importance whether the problem involves at-grade roadways, tunnels, or elevated structures. There are potential differences between these problems. The road traffic produces ground waves *on* the surface as well as *beneath* the surface. and these waves are fundamentally different in character. The tunnel represents a source of vibration

† An abbreviated version of this section has been published recently [9].

that in principle will also produce surface and body (interior) waves, although for a buried source the strength and behaviour of the surface wave is not well understood. It seems likely that, if buried deep enough, the tunnel will excite principally body waves, and that likelihood can often be exploited. Further, an elevated structure can produce surface waves that, in the far-field of an ideal transmission path, display no geometrical spreading losses.

It is worth noting that, of the literature available, a number of works contain excellent surveys of various facets of the problem and extensive lists of references. These include the reports of Crandall [3], Whiffin and Leonard [4], and Remington [10].

2.1. SOURCES AND SPREADING

The basis of almost all of the analytical work on sources and transmission paths in soils is contained within the pioneering work of Lamb who investigated the response of isotropic, homogeneous elastic half-spaces to various harmonic and impulsive loads. Indeed, although many special cases have been examined in the intervening years, the pattern of what can be done analytically lies along outlines developed in the early part of this century. By way of review, the principal features of the responses of an elastic half-space to point and line loads will be discussed briefly [1–3].

If an oscillating point load is applied to an otherwise unloaded elastic half-space, three types of waves will emanate from the loading point. One is a surface wave, termed a Rayleigh wave, whose horizontal and vertical amplitudes drop off exponentially with the co-ordinate normal to the surface, while, in the far field, it falls off with distance along the surface at a rate inversely proportional to the square root of the surface distance. The Rayleigh wave is the slowest of the three wave types, so it thus is the last to arrive at a remote surface station. The other two waves are termed body waves, one of which propagates at the longitudinal wave speed of an elastic solid, and whose vibrational motion is in the direction of propagation. The other body wave, a transverse wave, travels at the shear wave speed, which is intermediate between the longitudinal wave speed and the Rayleigh wave speed. Both body waves fall off in amplitude in a manner inversely proportional to the spherical distance from the source point when monitored in the interior of the elastic space. When monitored on the surface, the body wave amplitudes fall off in a manner inversely proportional to the square of the surface distance. Thus at large distances from the source point the body waves that will be seen at the half-space surface will be of much smaller amplitude than the Rayleigh surface waves. At points well below the surface, of course, the body waves are the predominant feature of the response. It is also of interest to note that, for a small rigid disk vibrating on a half-space surface, 67 % of the input energy goes into Rayleigh waves, 26 % into shear waves, and only 7 % goes into the longitudinal waves.

If a line load is applied to the half-space, the response is then typical of cylindrical energy spreading: that is, in the interior, the fall off in amplitude of body waves is inversely proportional to the square root of the radial distance to the line source. On the surface, body waves would fall off in amplitude in a manner inversely proportional to the radial distance. The Rayleigh (surface) waves in this instance do not fall off with distance along the surface, and, for an ideal (undamped) solid, progress out to infinity with unchanged amplitude.

For buried point and line loads or sources one would get, if the distance to the free surface is large enough for a far field to develop, the spherical and cylindrical spreading of the energy of body waves that is characteristic of the symmetries of such surfaces. Thus, for the point source, the amplitude of the waves falls off inversely as the spherical radial distance, while for the line load the amplitude is inversely proportional to the square root of the cylindrical radial distance. A buried source can also produce Rayleigh surface waves by reflection of the body waves at a free surface. Unless the source is very shallow, however, these surface waves will be relatively insignificant.

Now it ought to be noted that all of the above descriptions, which are summarized in Figure 1, are based on far-field analyses of elastic spaces, in responce to time-harmonic loads.

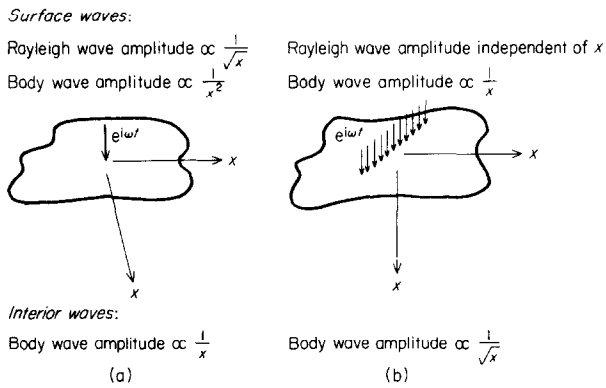

Figure 1. Summary of spreading attenuation characteristics for oscillating (a) point and (b) line loads applied to the surface of an elastic half-space.

Thus, energy dissipation is ignored (that subject is taken up in the next section), as are the non-propagating near fields of these various sources and of the possible time dependencies of the loading. However, as one is generally interested in frequency responses within small bandwidths, and as the time dependencies of the loads do not markedly change the geometric characteristics of the response, the above descriptions serve as adequate guides for most applications.

Traffic-induced vibration emanating from tunnels and at-grade roadways may normally be modeled as a line source. Where an elevated structure is involved, however, a receiver point may be in any one of several source fields, depending upon the location of that receiver relative to the superstructure and to the individual piers. Thus, near a pier, one must contend with propagation, both far-field and near-field, from a point source. As one moves away from the elevated highway, say along a line normal to its axis, the point source near-field becomes of less significance, and the individual (pier) point far-fields "coalesce" so as to be seen as the far-field of a line source. Of course, if one moves far enough away from an elevated highway of limited extent, that source can be viewed again as a point source. Similarly, a single machine (e.g., a pile driver) or a road surface irregularity such as a pot hole may be viewed as a point source.

Additionally, one always faces the problem of deciding what these field distances are, in relative terms. This means that one must be able to define a frequency band of interest and a

TABLE 1
Radiation (spreading) attenuation;
A_s = *spreading attenuation* = $S \log x/x_0$

Physical sources	Model	Wave	Monitor location	S
Highway/rail line	Line	Rayleigh	Surface	0
footing array		Body	Surface	20
Car in pothole,	Point	Rayleigh	Surface	10
single "el" footing		Body	Surface	40
Tunnel	Buried line	Body	Interior	10
Buried explosion	Buried point	Body	Interior	20

propagation wave speed, so that wavelengths can be calculated, which in turn allows appropriate comparison with source dimensions: e.g., the diameter of a pier footing and the spacing of piers. Spreading attenuation characteristics for practical physical sources are summarized in Table 1. In a later section some implications of applying these spreading formulae will be discussed in the light of current practice.

2.2. DAMPING PROPERTIES OF SOILS

This section is devoted to a discussion of the dynamic properties of various soils, particularly the damping (or energy dissipation) properties. This is an area where there is a dearth of hard information. There does seem to be reasonable information on longitudinal and shear wave speeds; there appears to be no consensus on the energy dissipation aspects.

It is generally agreed that the decay in amplitude can be represented in the form (for only the damping decay)

$$A(x) = A_0 e^{-\alpha x}. \tag{1}$$

The controversial issue is the frequency dependence of the absorption coefficient, α.

There appears to be little doubt that the damping must be frequency dependent, and the available data (e.g., see pp. 192–197 of reference [3], and pp. 25–27 of reference [7]), certainly bears this out. On the other hand, whereas Barkan [1] presents the arguments for a viscous model of damping in which absorption is dependent on the square of the frequency and for an elastic recovery model for dissipation in which absorption is linearly dependent on frequency, he also presents a table of values of absorption coefficients which are apparently independent of frequency! Some representative values are displayed in Table 2.

TABLE 2
Representative soil absorption coefficients [1]

	$\alpha(\text{ft}^{-1})$	$\alpha(\text{m}^{-1})$
Water–saturated clay	0·012–0·037	0·040–0·120
Loess and loessial soil	0·030	0·100
Sand and silt	0·012	0·040

With attenuation defined by the relation

$$A_T = -10 \log (A(x)/A(0))^2 \quad \text{(dB)}, \tag{2}$$

one can combine equations (1) and (2) to calculate the damping attenuation as

$$A_d = -10 \log e^{-2\alpha x} \quad \text{(dB)}, \tag{3}$$

which can be recast (by using standard properties of logarithms) in the form

$$A_d = -10\,(0{\cdot}434)(-2\alpha x) = 8{\cdot}68\alpha x \quad \text{(dB)}. \tag{4}$$

Then, for example, it is possible to compute for the soils listed above the values of attenuation (the smaller absorption coefficient is used for clay); these are shown in Table 3.

TABLE 3
Frequency-independent damping attenuation (calculated from data provided by Barkan [1])

x (ft)	100	150	200	300
A_d—clay (dB)	10·4	15·6	20·8	31·2
A_d—loess (dB)	26·0	39·0	52·0	78·0
A_d—sand (dB)	10·4	15·6	20·8	31·2

These are clearly very large values of attenuation, and it is difficult to accept them as being uniformly valid over all frequency ranges. The only support for this notion comes from two small experiments conducted by Barkan [1, p. 346] in which he determined that over the frequency range 10 Hz $< f <$ 30 Hz there was no substantial change in the absorption coefficient.

An alternate approach, one that yields considerably more conservative results, is to assume that the absorption coefficient is linearly dependent on frequency [3, 6]. Thus, one assumes that

$$\alpha = \pi\eta f/c, \tag{5}$$

where η is the (constant) loss factor and c is the appropriate wave speed: e.g., the longitudinal or shear speed, depending on the wave under consideration. The attenuation would then take the forms

$$A_d = -10\log e^{-2\eta\pi f x/c}, \tag{6}$$

$$A_d = 27{\cdot}29\eta f x/c. \tag{7}$$

For longitudinal waves, which decay more slowly because of the larger wave speed, values of the attenuation were calculated for $f = 4$ Hz, and these are given in Table 4. In the above calculation the loss factors used were 0·50 for clay, 0·30 for the loess, and 0·1 for the sand.

TABLE 4

Frequency-dependent (linear) damping attenuation calculated for longitudinal waves at 4 Hz

x (ft)	100	150	200	300
A_d—clay (dB)	1·1	1·7	2·2	3·3
A_d—loess (dB)	1·2	1·8	2·4	3·6
A_d—sand (dB)	0·7	1·0	1·4	2·0

The assumed longitudinal wave speeds were 5000 ft/s (1524 m/s) for clay, 2800 ft/s (853 m/s) for loess, and 1500 ft/s (457 m/s) for sand. Because of the linear dependence of frequency, the very low value of attenuation displayed above will become comparable to the values presented earlier at frequencies of 40 Hz and higher. An alternate presentation of the damping of soils, in terms of the number of wavelengths from the source, is displayed in Figure 2.

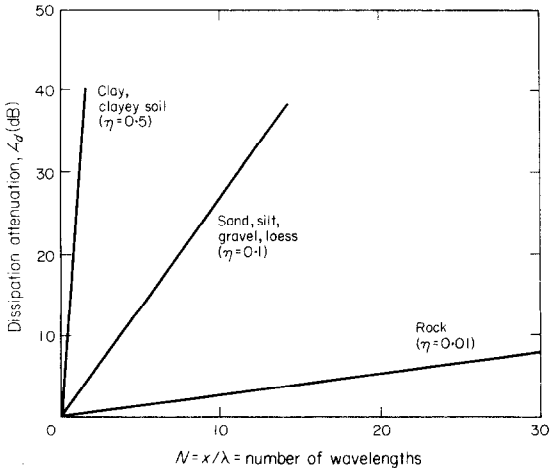

Figure 2. Summary of dissipation attenuation for various soils based on nominal soil properties given in reference [6]. $A_d = -10\log e^{-2\pi\eta(x/\lambda)} = 27{\cdot}29\eta(N)$.

However, it must be recognized here that for a conservative estimate of low frequency vibration impact, it is appropriate to assume that the damping attenuation is fairly small.

3. INSTRUMENTATION FOR GROUND VIBRATION MEASUREMENTS

This section is devoted to discussion of the principal types of instrumentation used to measure ground vibration. This review will be of value not only for its own sake, but will also assist in the interpretation of the data to be given in the next section.

Most of the ground vibration data that will be discussed in the following section have been obtained by using one of two general instrumentation systems. The first system, popular with geologists and civil engineers, and often applied to the measurement of ground motion generated by blasting and pile driving, is the seismograph. The second system, widely used by acoustical engineers for the measurement of railway and roadway induced ground vibration, may be called the vibration level meter, or VLM.

The primary difference between the two systems is that the seismograph displays actual ground motion, within the frequency and phase limits of the system, in the time domain, whereas data obtained with a VLM is most often displayed as an r.m.s. level in the frequency domain. It should be pointed out that one is not limited to one system or the other. In practice, depending upon the application, combinations of elements of the two systems can be used. However, as mentioned above, this discussion is limited to the systems that are most commonly used. The important differences and limitations, which will be discussed further below, are (1) frequency response of the system, (2) transducer type, size and coupling to the ground, (3) detection circuitry and (4) display.

3.1. SEISMOGRAPHS

The basic seismograph is comprised of a triaxial transducer, amplifiers, and oscillograph. The entire system may be self-contained in a single unit, or the transducer may be separate, connected to the amplifiers and recording unit by a cable. The data output of the seismograph is a time history, on paper tape, of the ground motion, usually as velocity, in three perpendicular directions. The normal convention used to describe the three components is r, radial (or sometimes l, longitudinal), v, vertical, and t, transverse. A typical seismograph record is shown in Figure 3. The time history signals shown in Figure 3 are linear in both amplitude and time. As can be seen, timing lines provide a reference for the determination of the principal frequency of motion. The amplitude is unrectified and the seismograph has been designed to represent the actual ground motion within the frequency, phase, and time response limits of the system.

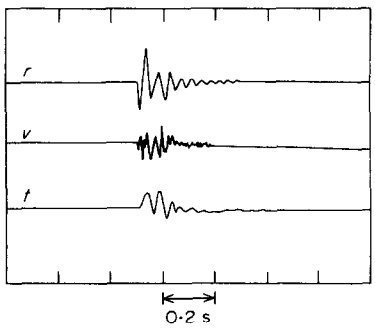

Figure 3. Time history velocity traces of blast vibration.

The frequency response of a typical seismograph is limited in the low frequency range by the transducer, and in the high frequency range by the oscillograph galvanometers. Generally the transducers operate above their natural frequency and are always highly damped. Common transducer resonance frequencies are between 2 Hz and 5 Hz with damping of some 55% to 70% of critical damping. The low frequency 3 dB down point can be estimated by the following equation:

$$f_{(-3\,\mathrm{dB})} = ((2\zeta_t^2 - 1) + \sqrt{(2\zeta_t^2 - 1)^2 + 1})^{1/2} f_t, \tag{8}$$

where f_t is the natural frequency of the transducer, and ζ_t is the transducer's critical damping ratio. For example, if $\zeta_t = 0{\cdot}6$ and $f_t = 2$ Hz, $f_{(-3\,\mathrm{dB})} = 1{\cdot}7$ Hz. Transducers of this type are limited in maximum displacement based on dimension and geometry considerations. A limitation of less than 1 inch is not uncommon. In theory, the seismic mass of the transducer should remain stationary while the transducer housing (which in some cases is the entire seismograph) will follow the motion of the ground.

It is obvious that at high frequencies the driving point impedance of the transducer housing will become significant when compared with the impedance of the ground. This usually occurs, however, at frequencies much higher than our typical range of interest. Some recent measurements of the absolute value of the driving point impedance of two different types of soils by White and Mannering [11] provide valuable data for estimating this effect. Equation (9) says that the measured velocity, V, will be different from the actual ground velocity, V_0, if the mass impedance of the seismograph, $j\omega m$, is similar to or greater than the driving point impedance of the soil, Z_s:

$$V = V_0 Z_s/(Z_s + j\omega m). \tag{9}$$

If one assumes a single unit seismograph of 35 lb, and uses this result of White and Mannering, who give a soil impedance at 100 Hz of approximately 570 $\frac{\text{lb·s}}{\text{in}}$ (10^5 $\frac{(\text{N·s})}{\text{m}}$ for both sand and clay, and assumes that Z_s has the phase of a spring impedance [3], one then finds the measured velocity as $V = 1{\cdot}1\,V_0$. Nevertheless, newer portable seismographs incorporate separate transducers which weigh much less than the seismograph mentioned above. In fact, some modern seismographs are designed with a transducer density similar to average soil densities to minimize transducer mounting problems.

The high frequency response of the seismograph is limited by the oscillograph galvanometers. The 3 dB down point can be estimated by the following equation:

$$f_{(-3\,\mathrm{dB})} = ((1 - 2\zeta_g^2) + \sqrt{(1 - 2\zeta_g^2)^2 + 1})^{1/2} f_g, \tag{10}$$

where ζ_g is the critical damping ratio for the galvanometer, and f_g is the galvanometer's natural frequency. A typical seismograph might have galvanometers with characteristics of $f_g = 200$ Hz and $\zeta_g = 0{\cdot}6$. In this case the useful frequency response would extend out to approximately 230 Hz. Note that for $\zeta_g = 1/\sqrt{2}$, $f_{(-3\,\mathrm{dB})} = f_g$. Figure 4 shows the frequency response characteristics of a popular seismograph.

3.2. VIBRATION LEVEL METERS

The other systems which are widely used to measure ground vibration are those which are here called vibration level meters (VLM). These systems do not come in single unit packages, such as seismographs, but instead are comprised of a collection of equipment which may vary widely in characteristics. Still, there are certain standard elements to the VLM which are discussed here. In general the VLM system is similar to equipment used for acoustical measurements, but with a much lower frequency response.

A general system which might be used to measure low level, low frequency ground motion would incorporate a high sensitivity piezoelectric accelerometer, voltage preamplifier and low

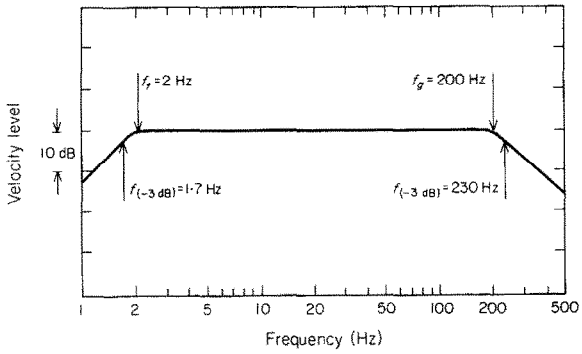

Figure 4. Frequency response of a seismograph.

pass filter, second amplification stage with 1/3-octave band filters, and an r.m.s. rectifier and logarithmic display. Data can be directly obtained from this system or recorded on magnetic tape either by using an FM recorder or by speed scaling on an AM recorder. Tape recorded data can then, of course, be analyzed in either the time domain or the frequency domain, or both.

The low frequency response of the VLM is limited by the electrical damping constant created by the preamplifier resistance, R, and the total capacitance, C, of the preamplifier, cable and accelerometer. The 3 dB down point can be calculated from the familiar formula

$$f_{(-3\,dB)} = 1/2\pi RC. \tag{11}$$

By properly selecting the accelerometer and preamplifier, the low frequency response can be extended down to the limitations imposed by the amplifier. In general, popular amplifier units used as part of a VLM are limited in the low frequency response below about 2 Hz. Accelerometers operate below their natural frequencies, which may vary from 500 Hz to 50 kHz, and they are generally lightly damped. Therefore, to avoid high frequency overloading and to improve the signal-to-noise ratio, a low pass filter is often employed. A simple filter which drops off at 6 dB per octave above 250 Hz would be capable of eliminating the resonance effects of most, but not all, accelerometers.

To measure vibration which has extremely low amplitudes, a very sensitive accelerometer must be employed and a noise floor measurement (either by isolating the accelerometer or by using an equivalent capacitance dummy transducer) should be made. By properly selecting components, one can assemble a VLM capable of measuring levels well below the human threshold of perception for whole body vibration. (It should be noted that equally sensitive seismographs are also available.) It is also worth noting that most VLM measurements are made in one direction at a time; triaxial accelerometers are available but would require three separate amplification channels.

There are no standard ground mounting techniques for accelerometers. Seismographs, if they are the single unit type, are merely leveled on the ground, and if the acceleration does not approach something less than 1 g, respond with the ground motion within the limits mentioned above. For the newer seismographs, with matching soil density transducers, a small hole is excavated and the transducer is buried in it. The accelerometers discussed here are much smaller than the transducers used with seismographs. The advantages of a small accelerometer for measuring vibration of lightweight structures are of little benefit for measuring ground vibration. In fact, accelerometers are generally attached to a larger structure such as a wedge, a rod, or a plate, which in turn is secured to the ground. Of course, these larger structures must be selected with care to insure good coupling to the ground while avoiding the point impedance problem mentioned earlier.

Data is most often displayed as the r.m.s. acceleration level on the logarithmic face of the

VLM. The ratio between the peak level and r.m.s. level of an oscillatory motion is called the crest factor. The crest factor must be known or estimated to compare data from the VLM with that from the seismograph. For sinusoidal motion it is well known that the crest factor is 1·414 or 3 dB; however, for random vibration, and in particular for impact, the crest factor may be on the order of 5 to 20 dB. For impulsive vibration with large crest factors there are two problems that may arise when an r.m.s. meter is used: (1) the input amplifiers may be overloaded even when the r.m.s. meter reading is on scale; and (2) the (statistical) confidence in the displayed r.m.s. value decreases rapidly as the signal duration decreases. This latter point is particularly important for narrow band analysis. To avoid these problems, which principally occur for impact measurements, one should select a peak reading meter rather than an rms meter. For the types of vibration measurements discussed here this refers primarily to blast and pile driving generated vibration.

Figure 5 shows the frequency response for the typical VLM system discussed above.

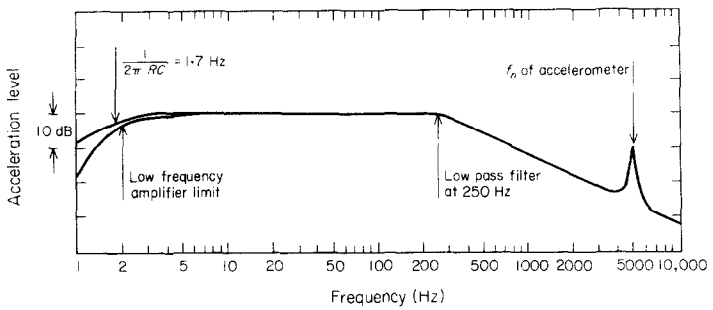

Figure 5. Frequency response of a vibration level meter.

4. MEASUREMENTS OF GROUND VIBRATION ATTENUATION

The propagation of man-made ground vibration in the frequency range of 1 to 200 Hz has been of interest to scientists and engineers for some time. In particular, considerable data has been obtained for vibration generated by blast and by pile driving. More recently, attention has been turned to the problems of vibration induced by rail and roadway traffic. Generally this data has been obtained to predict or avoid vibration effects such as building damage, perceptible motion, interference with sensitive equipment, radiated sound, and soil settlement. The instrumentation chosen to measure ground vibration depends largely on the particular effects to be studied, the wave characteristics and the governing criteria. For example, the U.S. Bureau of Mines has published a "safe blasting limit" in terms of "peak particle velocity as measured from any of three mutually perpendicular directions in the ground adjacent to a structure" to avoid major and minor structural damage [12]. In this case a three-channel peak-reading velocity meter with a triaxial transducer is required. The seismograph mentioned earlier is ideally suited for these types of measurements.

On the other hand if the issue is human perception of ground motion, and if the motion is expected to be broad band in nature, one would employ an instrument capable of frequency analysis, such as the vibration level meter. This is due to the frequency dependence of the human threshold of perception to whole body vibration. (It should be noted that over certain frequency ranges the human threshold can be approximated by a constant velocity [13].)

4.1. BLAST GENERATED VIBRATION

In Bulletin 656 [12], the U.S. Bureau of Mines analyzed vibration data obtained for 171 blasts at 26 quarry sites to determine, among other things, a propagation law for groundborne

surface vibration. The instrumentation used had characteristics similar to those of a seismograph. While some spectral analysis was performed, in general the quantity sought was the peak particle ground velocity. A propagation law of the form

$$V = kx^{\beta} \tag{12}$$

was assumed, where V is peak particle velocity, x is distance, and k and β are constants which were determined by a standard regression analysis. It was determined that the propagation laws for the three orthogonal directions, r, v and t, were statistically different and required separate descriptions. The resulting propagation laws are

$$V_r = k_r x^{-1\cdot63}, \tag{13}$$

$$V_v = k_v x^{-1\cdot73}, \tag{14}$$

$$V_t = k_t x^{-1\cdot28}. \tag{15}$$

The standard error estimates for the three coefficients above are $S_{v_r} = 0{\cdot}0043$, $S_{v_v} = 0{\cdot}0049$ and $S_{v_t} = 0{\cdot}0063$. The geological conditions at transducer locations varied greatly, ranging from exposed bedrock to 56 ft (17 m) of overburden.

4.2. VIBRATION DUE TO PILE DRIVING

In pile driving vibration, as in blast generated vibration, the quantity sought is often peak particle velocity. In this case it is almost always true that the vertical vibration component will greatly exceed the radical and transverse components. (This, of course, cannot be generally stated for blast generated ground motion.) Consequently, it is the vertical component which is of primary interest in piling vibration. Again a propagation law of the form given in equation (12) is assumed, and the specific constants are determined by regression analysis. (When the results from various pile drivers are compared, it is the scaled distance $x/\sqrt{E}$ where E is the energy rating of the driver, that is plotted against peak velocity.) Measurements reported by Attewell and Farmer [14] for a wide variety of soil types, including both sandy and clayey soils, best fit a curve of the form

$$V = kx^{-0\cdot87}. \tag{16}$$

These authors go on to argue that their data and that of others suggest that $\beta = -1{\cdot}0$ is a good approximation over a wide variety of soil types. One other interesting result presented in that paper can be seen in the profiles of surface wave particle motion at 33 ft (10 m), 66 ft (20 m) and 98 ft (30 m) from a driven sheet pile. As might be expected, there is considerable confusion at 33 ft; however, by 98 ft a very clear retrograde ellipitcal pattern, typical of Rayleigh waves, can be seen. These results, however, do not agree entirely with typical vertical motion time histories given elsewhere in the paper. These traces show a clear separation between the body wave arrivals and the Rayleigh wave arrival at a position as close as 16 ft (5 m) from a driven sheet pile. It is also interesting to note that the velocity amplitude of the Rayleigh wave is nearly 6 times as large as the body wave amplitude at this same distance.

One might readily conclude that pile driving excites primarily Rayleigh waves. It is then evident that to obtain a propagation law coefficient of $\beta = -1{\cdot}0$, considerable energy must be lost to internal dissipation. In this case spreading losses alone would result in $\beta = -0{\cdot}5$.

Additional results for a large number of pile driving measurements are given by Wiss [15], who found different propagation laws for different soil types. For wet and dry sand, Wiss suggests a propagation law of the form

$$V = kx^{-1\cdot0}. \tag{17}$$

On the other hand, in clay, ground motion was found to decay more rapidly with distance, and the suggested propagation law is

$$V = kx^{-1\cdot5}. \tag{18}$$

Both Wiss [15] and Attewell and Farmer [14] mention that for most sandy and clayey soils the principal frequency of vibration due to pile driving is generally found between 15 and 35 Hz. No mention is made by any of these authors as to whether the principal frequency shifts down as distance from the pile is increased. Such behavior would be expected, of course, if the spectrum were rather broad and if the soil damping were frequency dependent. Such behavior has been reported for traffic induced vibration by Whiffin and Leonard [4].

4.3. TRAFFIC AND RAIL GENERATED VIBRATION

Vibration generated along a road or railway can be (geometrically) modeled as a line source provided that the roadway surface is relatively uniform, and provided that the receiver is in the far field of the source, but less than approximately $1/\pi$ times the length of the roadway or train†. In this case, if the assumption is made that the predominant ground motion is due to Rayleigh waves, there will be no spreading loss and any vibration attenuation will be due to soil damping.

Based on these assumptions, vibration data at various distances from an elevated structure [7] and from an at-grade highway [8] is plotted as attenuation (A_d) *versus* the distance in wave lengths (x/λ) in Figures 6 and 7. If A_d were proportional to frequency one would expect the straight line relationships for the nominal soil values shown in Figure 2. However, the data

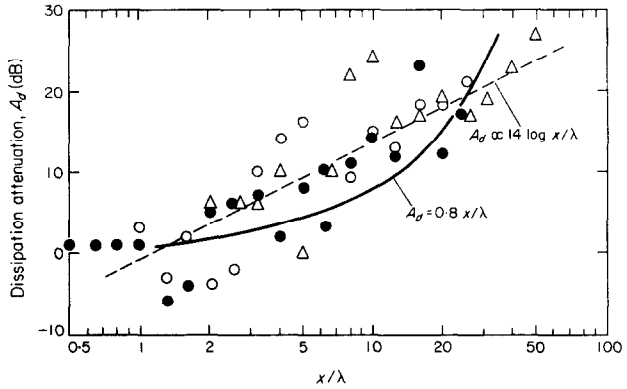

Figure 6. Dissipation attenuation in saturated clay, based on data taken near an elevated highway structure [7]. ●, $x = 100$ ft; ○, $x = 200$ ft; △, $x = 400$ ft.

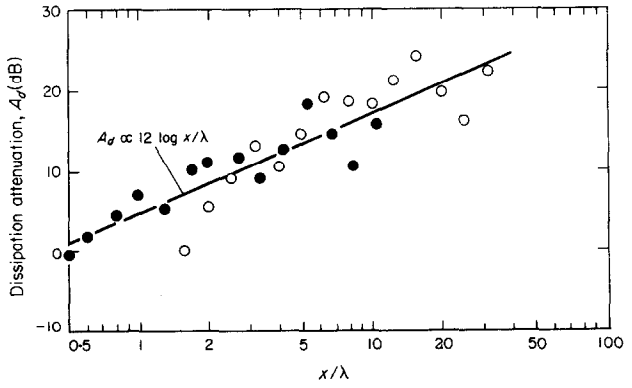

Figure 7. Dissipation attenuation in dry sand, based on data taken near an at-grade highway [8]. ●, $x = 100$ ft; ○, $x = 300$ ft.

† Rathe [16] has calculated the cross-over point where a finite acoustic line source begins to look like a point source. While this calculation does not apply directly to R-waves, a similar calculation will show a cross-over near the distance of $1/\pi$ times the source length.

shown in Figures 6 and 7 lines up quite well when plotted on semi-logarithmic paper, indicating a logarithmic rather than linear relationship.

The data shown in Figure 6 was obtained by Hanson, Remington and Gutowski [7] at various distances from an elevated highway structure. The measurements were made by using a VLM type system. The transducer was mounted to a 4 in × 4 in × ¼ in (10 cm × 10 cm × 0·6 cm) thick aluminum plate which was pressed into the saturated clay soil. Data obtained with this mounting technique was compared to results found by mounting the accelerometer on top of a 1 in × 1 in × 6 in (2·5 cm × 2·5 cm × 15 cm) long steel rod driven into the ground. When located at the same distance from a highway footing, the two mounting techniques, monitored simultaneously, were found to give readings within ± 1·5 dB of one another over a frequency range of 2·5 Hz to 250 Hz.

The attenuation values shown in Figure 6 represent the difference between the L_{10}† of the rms peaks measured at 2 ft (0·6 m) and 100 ft (30 m), 200 ft (61 m), and 400 ft (122 m). To compute x/λ, a Rayleigh wave speed of 500 ft/s (152 m/s) was assumed.

Both linear and logarithmic curves were fitted to the data and it is readily apparent from the mathematics as well as straight-forward observation that a logarithmic curve gives a better fit. Note that the logarithmic curve appears as a straight line on the semi-logarithmic plot, while the linear curve, which was forced through the point $x/\lambda = 0$, $A_d = 0$, actually appears curved. The resulting attenuation formulae and coefficents of correlation (r) then appear as follows:

$$A_d = 0{\cdot}8x/\lambda \qquad (r = 0{\cdot}68), \tag{19}$$

$$A_d = 14 \log x/\lambda \qquad (r = 0{\cdot}86). \tag{20}$$

The corresponding loss factor for equation (19) is $\eta = 0{\cdot}03$.

It can also be observed in Figure 6 that the linear fit predicts more conservative attenuation values out to $x = 25\lambda$, and that the two curves are within ± 5·5 dB from $x = \lambda$ to 34λ. The trend of the data displayed in Figure 6 suggests a number of possibilities. It may well be that ground damping is non-linear: at close distances to the source, where the vibration amplitudes are large, there is more attenuation per wave length than at farther distances (smaller amplitudes). On the other hand, it may be that soil damping is linear, but at large distances strata or soil inhomogeneities reflect or scatter waves (body or Rayleigh) to the surface.

This same trend can be seen in Figure 7. The attenuation values, derived from data reported by Blazier [8], are the difference in median rms acceleration levels at 100 ft (30 m), 200 ft (61 m) and 400 ft (122 m) from an at-grade highway. In these calculations, a Rayleigh wave speed of 600 ft/s (183 m/s) was assumed. This attenuation data is best fitted by a logarithmic curve of the form $A_d = 12 \log x/\lambda$. The coefficient of correlation is $r = 0{\cdot}90$.

4.4. STEADY STATE, POINT SOURCE VIBRATION

Two recent studies provide additional information concerning the attenuation of ground vibration with distance. Murray [17] has recently investigated the propagation of vibration signals in alluvial fill, due to heavy machinery oscillation. His data has been plotted in Figure 8 as the difference in rms acceleration levels at 1 ft (0·3 m) and at distances ranging from 9 ft (3 m) to 2000 ft (610 m). In order to show attenuation due to dissipation only, Murray's data was first adjusted for spreading loss by a term −10log distance, appropriate for a point Rayleigh wave source. Further, a Rayleigh wave speed of 600 ft/s (183 m/s) was assumed. Murray's data was fitted by a curve of the form $A_d \propto 11 \log x/\lambda$. The coefficient of correlation for this curve is $r = 0{\cdot}70$.

White and Mannering [11] report the results of a series of measurements in which vibration

† The vibration level that is equalled or exceeded by 10% of the measured peaks.

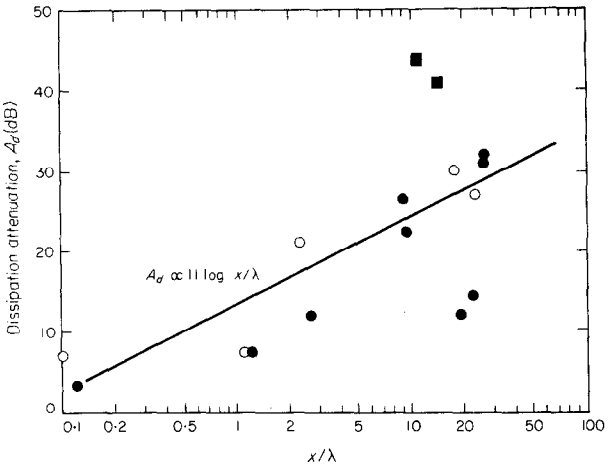

Figure 8. Dissipation attenuation in alluvial fill, based on data taken near a heavy machine [17]. ●, $f = 7{\cdot}8$ Hz, on fill; ■, $f = 7{\cdot}8$ Hz, on bedrock; ○, $f = 7{\cdot}0$ Hz, on fill.

attenuation and soil impedance values, which were previously mentioned, are given. Data for both London clay, with a measured Rayleigh wave speed of 466 ft/s (142 m/s) and for Barton sand (wave speed not given) are presented. The authors point out that significant harmonic distortion was observed next to the source when the ground was driven with a sinusoidal vibrator at 40 Hz. There is no mention of the magnitude of the driving force, nor of the linearity of the vibrator itself; the harmonic distortion is attributed to non-linear soil behavior. Ground attenuation values are given for impacting and steady state point sources, with roughly similar results, for London clay. The steady state values, shown in Figure 9, have been adjusted to give only attenuation due to dissipation. The results at 246 ft (75 m)

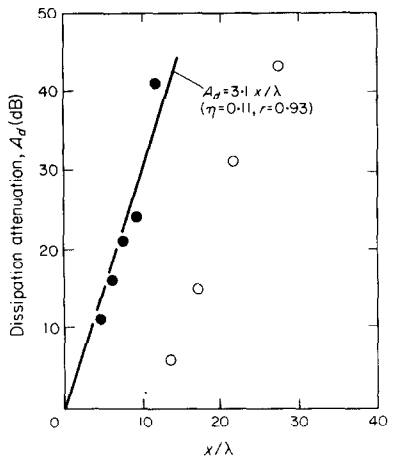

Figure 9. Dissipation attenuation in London clay, based on experimental data [11]. ●, $x = 82$ ft; ○, $x = 246$ ft.

show very peculiar behavior, suggesting perhaps soil non-linearities. In Figure 10 the dissipation attenuation, A_d, *versus* x/λ, assuming a Rayleigh wave speed of 800 ft/s (244 m/s) for sand is shown. The resulting soil loss factors for London clay at 82 ft (25 m), and Barton sand are $\eta = 0{\cdot}11$ and $\eta = 0{\cdot}07$, respectively. The least squared curves and coefficients of correlation are shown in the figures.

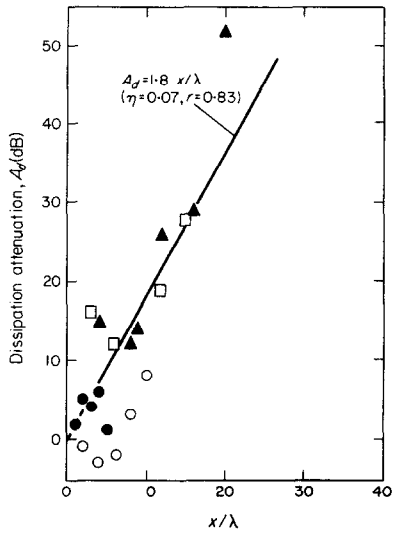

Figure 10. Dissipation attenuation in Barton sand, based on experimental data [11]. ●, $x = 82$ ft; ○, $x = 164$ ft; □, $x = 246$ ft; ▲, $x = 328$ ft.

5. CONCLUSIONS

There is much to be learned from the information presented in the preceding sections. Perhaps most important is the fact that the simple prediction models are not by themselves adequate for any serious purpose. This, in turn, is due to the wide variation in predicted attenuation values for soils of nominally similar (verbally, at least) descriptions. On the other hand, the empirical data itself may be questioned, for there is no *standard* measurement procedure. Thus, for serious practical work, the optimum approach will combine very careful measurement with seasoned analytical judgment.

In spite of these drawbacks, however, there still are many ground vibration problems for which one cannot afford extensive individual measurements and yet requires certain tentative conclusions for guidance. For such cases, based on the results previously reviewed, a graphical summary displaying expected dissipation attenuation for various soil types is presented as Figure 11. These curves may be viewed as an alternative to the straightforward application of the ideal models presented earlier in this paper.

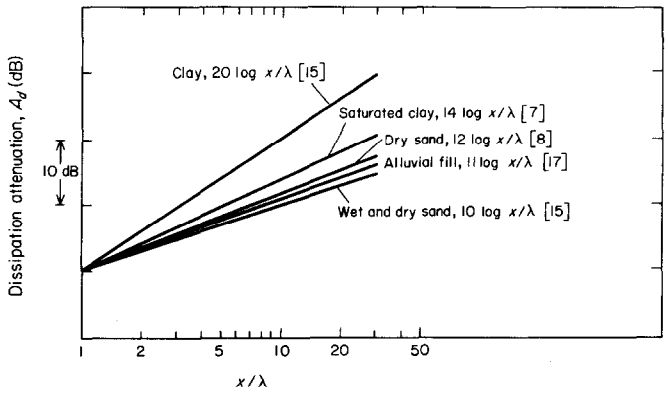

Figure 11. Summary of dissipation attenuation data for various soils.

REFERENCES

1. D. D. BARKAN 1962 *Dynamics of Bases and Foundations*. New York: McGraw-Hill Book Company, Inc.
2. F. E. RICHART, JR, T. R. HALL, JR and R. D. WOODS 1970 *Vibrations of Soils and Foundations*. Englewood Cliffs, New Jersey: Prentice-Hall, Inc.
3. S. H. CRANDALL 1974 in *Prediction and Control of Rail Transit Noise and Vibration* (J. E. Manning, R. G. Gann and J. J. Freidberg, U.S. Department of Transportation, Report No. PB 233 633). Propagation of noise and vibration through soil.
4. A. C. WHIFFIN and D. R. LEONARD 1971 *Road Research Laboratory Report LR* 418. A survey of traffic-induced vibrations.
5. T. K. LIU, E. B. KINNER and M. K. YEGIAN 1974 *Sound and Vibration* **8**, 26–32. Ground vibrations.
6. E. E. UNGAR and E. K. BENDER 1973 *Bolt Beranek and Newman Inc. Report* 2500*B*. Guidelines for the preliminary estimation of vibrations and noise in buildings near subways.
7. C. E. HANSON, P. J. REMINGTON and T. G. GUTOWSKI 1973 *Bolt Beranek and Newman Inc. Report* 2635. Measurement, prediction and assessment of traffic-generated vibrations from the proposed I-10/Carrollton Avenue, overpass, New Orleans.
8. W. E. BLAZIER, JR 1968 *Bolt Beranek and Newman Inc. Report* 1752. An estimate of ground vibration levels at the proposed site for IBM (San Jose) building 028 due to vehicular traffic on the future West Valley freeway.
9. C. L. DYM 1976 *Sound and Vibration* **10**, 32–34. Attenuation of ground vibration.
10. P. J. REMINGTON *et al.* 1974 *Bolt Beranek and Newman Inc. Proposal P74-PSD-92*. Determination of impact from vibrations related to highway use.
11. R. G. WHITE and M. E. J. MANNERING 1975 *Journal of the Society of Environmental Engineers* **14-1**, 3–9. Techniques for measuring the vibration transmission characteristics of the ground.
12. H. R. NICHOLLS, C. F. JOHNSON and W. I. DUVALL 1971 *U.S. Bureau of Mines Bulletin* 656. Blasting vibrations and their effects on structures.
13. T. MIWA 1967 *Industrial Health* **5**, 183–205. Evaluation methods for vibration effect: Part I Measurements of threshold and equal sensation contours of whole body for vertical and horizontal vibrations.
14. P. B. ATTEWELL and I. W. FARMER (undated) *Ground Engineering*, pp. 26–29. Modern piling Part Two: Attenuation of ground vibrations from pile driving.
15. J. F. WISS 1967 *Highway Research Record*, No. 155, 14–20. Damage effects of pile driving vibration.
16. E. J. RATHE 1969 *Journal of Sound and Vibration* **10**, 472–479. Note on two common problems of sound propagation.
17. F. M. MURRAY (to appear) *Noise Control Engineering*. Machinery foundation vibration: a case study of community annoyance.